[5-5]Bitrovacene, (μ-η^5:η^5-Fulvalenediyl)bis[(η^7-cycloheptatrienyl)vanadium]: Synthesis, Structure, and Intermetallic Communication[1]

Christoph Elschenbroich,* Olav Schiemann, Olaf Burghaus, Klaus Harms, and Jürgen Pebler

Fachbereich Chemie der Philipps-Universität, D-35032 Marburg, Germany

Received March 30, 1999

Lithiation of trovacene, (η^7-C_7H_7)V(η^5-C_5H_5), Li/I exchange, and Pd(dppf)Cl_2-catalyzed homocoupling affords [5-5]bitrovacene $\mathbf{5}^{2\bullet}$. Intermetallic communication manifests itself in typical biradical features of the EPR spectrum and in the resolution of redox splittings of 147 mV for the two subsequent oxidations and 224 mV for the reductions, respectively. $\mathbf{5}^{2\bullet}$ adopts a trans conformation in the single crystal (X-ray diffraction) as well as in rigid solution (EPR spectroscopy). A magnetic susceptibility study of $\mathbf{5}^{2\bullet}$ reveals weak antiferromagnetic coupling ($J = -2.78$ cm^{-1}) of the two V(d^5) centers.

Introduction

Among studies concerned with metal−metal interactions in dinuclear complexes, metallocenes as building blocks have played a prominent role. Major contributions came from the groups of Cowan[2], Hendrickson[3], Smart,[4] Köhler,[5] and Schottenberger;[6] the subject has been reviewed.[7] Our own efforts in this area have focused on bis(arene)metal units linked together either directly[8] or separated by a spacer.[9] Recently, we extended our studies to (η^7-tropylium)vanadium η^5-cyclopentadienyl (**1**$^\bullet$; trovacene), the unsymmetrical isomer of bis(η^6-benzene)vanadium (**2**$^\bullet$).[1,10] Compared to **2**$^\bullet$, **1**$^\bullet$ features a number of advantages which include (1) a pronounced anodic shift of the redox potential, $E_{1/2}$(**1**;+/0) = +0.26 V relative to $E_{1/2}$(**2**;+/0) = −0.35 V, which renders **1**$^\bullet$ almost air stable,[11] (2) the ease of functionalization, which is based on the fact that trovacene (**1**$^\bullet$) is selectively lithiated at the cyclopentadienyl ligand,[12] and (3) the orbitally nondegenerate ground state $^2A_1$ for the neutral V(d^5) complex **1**$^\bullet$, which contrasts with the isoelectronic ferrocenium ion (Fe(d^5), $^2E_1$) and furnishes well-resolved EPR spectra even at ambient temperature.

Chart 1

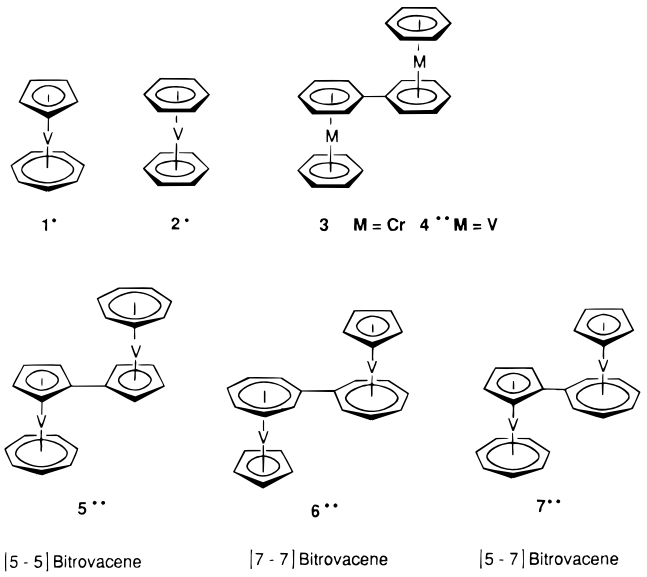

An attractive feature of the series **4**$^{2\bullet}$−**7**$^{2\bullet}$ (Chart 1) would be a comparative study of the propensity of the

* To whom correspondence should be addressed. E-mail: eb@ps1515.chemie.uni-marburg.de.

(1) Trovacene Chemistry. 2. Part 1: Elschenbroich, C.; Schiemann, O.; Burghaus, O.; Harms, K. *J. Am. Chem. Soc.* **1997**, *119*, 7452. The numbers in brackets indicate the site of substitution: [5]trovacene is functionalized at the cyclopentadienyl and [7]trovacene at the cycloheptatrienyl ligand.

(2) Cowan, D. O. *Acc. Chem. Res.* **1973**, *6*, 1. LeVanda, C.; Bechgaard, K.; Cowan, D. O.; Mueller-Westerhoff, U. T.; Eilbracht, P.; Candela, G. A.; Collins, R. L. *J. Am. Chem. Soc.* **1976**, *98*, 3181.

(3) Webb, R. J.; Geib, S. J.; Staley, D. L.; Rheingold, A. L.; Hendrickson, D. N. *J. Am. Chem. Soc.* **1990**, *112*, 5031.

(4) Smart, J. C.; Pinsky, B. L. *J. Am. Chem. Soc.* **1980**, *103*, 1009.

(5) Köhler, F. H.; Doll, M. H.; Prössdorf, W.; Müller, J. *Angew. Chem., Int. Ed. Engl.* **1982**, *21*, 151. Hudeczek, P.; Köhler, F. H. *Organometallics* **1992**, *11*, 1773. Hudeczek, P.; Köhler, F. H.; Bergerat, P.; Kahn, O. *Chem. Eur. J.* **1999**, *5*, 70.

(6) Schottenberger, H.; Buchmeiser, M.; Rieker, C.; Jaitner, P.; Wurst, K. *J. Organomet. Chem.* **1997**, *541*, 249.

(7) Barlow, S.; O'Hare, D. *Chem. Rev.* **1997**, *97*, 637. Astruc, D. *Acc. Chem. Res.* **1997**, *30*, 383.

(8) (a) Elschenbroich, C.; Heck, J. *Angew. Chem., Int. Ed. Engl.* **1977**, *16*, 479. (b) Elschenbroich, C.; Heck, J. *J. Am. Chem. Soc.* **1979**, *101*, 6773. (c) Elschenbroich, C.; Heck, J.; Massa, W.; Birkhahn, M. *Chem. Ber.* **1990**, *123*, 2321. (d) Elschenbroich, C.; Heck, J. *Angew. Chem., Int. Ed. Engl.* **1981**, *20*, 267.

(9) (a) Elschenbroich, C.; Heikenfeld, G.; Wünsch, M.; Massa, W.; Baum, G. *Angew. Chem., Int. Ed. Engl.* **1988**, *27*, 414. (b) Elschenbroich, C.; Bretschneider-Hurley, A.; Hurley, J.; Massa, W.; Wocadlo, S.; Pebler, J.; Reijerse, E. *Inorg. Chem.* **1993**, *32*, 5421. (c) Elschenbroich, C.; Metz, B.; Neumüller, B.; Reijerse, E. *Organometallics* **1994**, *13*, 5072. (d) Elschenbroich, C.; Bretschneider-Hurley, A.; Hurley, J.; Behrendt, A.; Massa, W.; Wocadlo, S.; Reijerse, E. *Inorg. Chem.* **1995**, *34*, 743.

(10) (a) Wolf, M. Ph.D. Thesis, Philipps-Universität, Marburg, Germany, 1998. (b) Plackmeyer, J. Diploma Thesis, Philipps-Universität, Marburg, Germany, 1998. (c) Schiemann, O. Ph.D. Thesis, Philipps-Universität, Marburg, Germany, 1998.

(11) Elschenbroich, C.; Bilger, E.; Metz, B. *Organometallics* **1991**, *10*, 2823.

(12) Groenenboom, J. C.; Liefde Meijer, H. J.; Jellinek, F. *Recl. Trav. Chim. Pays-Bas* **1974**, *93*, 6. Groenenboom, J. C.; Liefde Meijer, H. J.; Jellinek, F. *J. Organomet. Chem.* **1974**, *69*, 235.

10.1021/om9902232 CCC: $18.00
Publication on Web 07/23/1999

Scheme 1

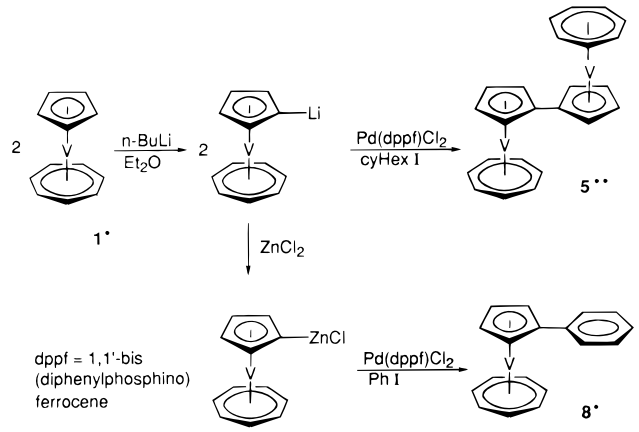

bridges μ-η^6:η^6-biphenyl, μ-η^5:η^5-fulvalenediyl, μ-η^7:η^7-heptafulvalenediyl, and μ-η^5:η^7-sesquifulvalenediyl to act as mediators between two V(d^5) half-sandwich units. We have studied compounds $\mathbf{3}^{2\bullet}$ [8a−c] (and $\mathbf{4}^{2\bullet}$ [8d]) previously; none of the species $\mathbf{5}^{2\bullet}$−$\mathbf{7}^{2\bullet}$ has been prepared as yet. In this communication we report on the synthesis of [5-5]bitrovacene ($\mathbf{5}^{2\bullet}$) and on its electrochemical, magnetic, and EPR spectroscopic properties.[13]

Results and Discussion

[5−5]Bitrovacene ($\mathbf{5}^{2\bullet}$) is obtained via lithiation, Li/I exchange, and Pd(dppf)Cl_2-catalyzed homocoupling as a violet, crystalline material which is soluble in toluene and tetrahydrofuran (Scheme 1). Intermediary transmetalation of [5]trovacenyl−Li to [5]trovacenyl−ZnCl and cross-coupling with iodobenzene affords phenyl−[5]trovacene (**8**•), which we prepared as a mononuclear reference molecule. The yield of $\mathbf{5}^{2\bullet}$ is limited by the, as yet unexplained, fact that lithiation of **1**• stops at 50% conversion.

$\mathbf{5}^{2\bullet}$ and **8**• have been subjected to X-ray crystal analyses; views of the structures are shown in Figures 1 and 2, and important bond lengths and angles are listed in the captions. Just like the related dinuclear complex (μ-η^6:η^6-biphenyl)bis[(η^6-benzene)chromium] (**3**),[8c] in the crystal $\mathbf{5}^{2\bullet}$ adopts an exact trans conformation, no deviations of the μ-fulvalenediyl bridging ligand from planarity and of the sandwich axes from a parallel orientation being present. A considerable twist angle of 24.2° is, however, observed between the η^5-C_5H_4 and the C_6H_5 planes in phenyl−[5]trovacene (**8**•). The lengths of the C−C bonds connecting the η^5-cyclopentadienyl ligand to its congener or to the phenyl substituent amount to 1.468 ($\mathbf{5}^{2\bullet}$) and 1.478 Å (**8**•), respectively; they mimic the respective parameter for **3** (1.483 Å[8c]) and for the free ligand biphenyl (1.493 Å[14]).

Intramolecular communication between two moieties in identical environments may in principle be inferred (1) from the redox splitting $\delta E_{1/2}$, i.e., the separation of the potentials of subsequent redox steps, (2) the hyperfine pattern in the EPR spectrum of a mixed-valence species, provided this is accessible under the limitations

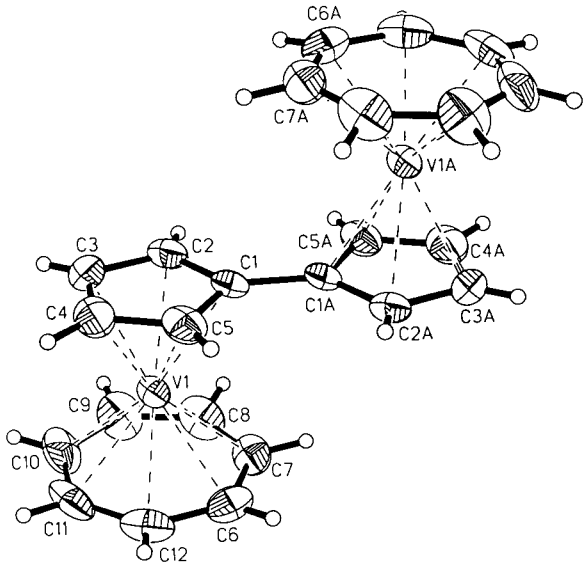

Figure 1. Molecular structure of [5-5]bitrovacene ($\mathbf{5}^{2\bullet}$) in the crystal (XP drawing and numbering scheme; ellipsoids are drawn at the 50% level). Selected bond lengths (Å) and bond angles (deg): V1−C1 = 2.281(2), V1−C2 = 2.248(3), V1−C3 = 2.235(3), V1−C4 = 2.242(3), V1−C5 = 2.265(3), V1−C6 = 2.168(3), V1−C7 = 2.174(3), V1−C8 = 2.178(3), V1−C9 = 2.178(3), V1−C10 = 2.186(3), V1−C11 = 2.173(3), V1−C12 = 2.162(3), C_5(centroid)−V = 1.912(5), C_7(centroid)−V = 1.465(1), C−C (mean for C_5) = 1.406(2), C−C (mean for C_7) = 1.394(2), C1−C1′ = 1.468(5), V1−V1′ = 5.501(1); dihedral angle C_5,C_5′ 0.00.

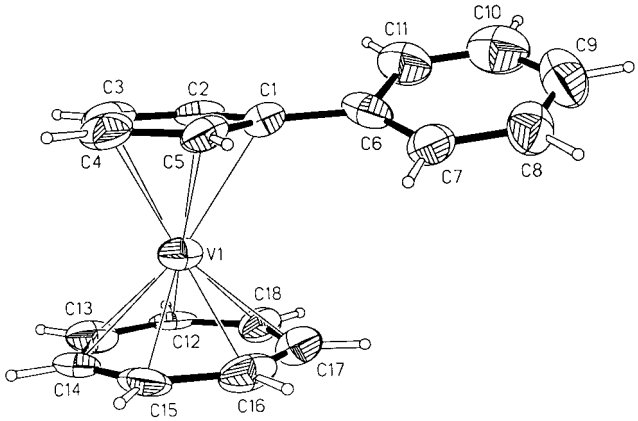

Figure 2. Molecular structure of phenyl−[5]trovacene (**8**•) in the crystal (XP drawing and numbering scheme; ellipsoids are drawn at the 50% level). Selected bond lengths (Å) and bond angles (deg): V1−C1 = 2.291(10), V1−C2 = 2.235(10), V1−C3 = 2.252(11), V1−C4 = 2.255(11), V1−C5 = 2.250(12), V1−C12 = 2.169(9), V1−C13 = 2.176(11), V1−C14 = 2.178(12), V1−C15 = 2.180(1), C1−C16 = 2.158(9), V1−C17 = 2.204(11), V1−C18 = 2.196(10), C_5(centroid)−V1 = 1.907(5), C_7(centroid)−V1 = 1.450(1), CC−C (mean for C_5) = 1.423(7), C−C (mean for C_7) = 1.412(6), C1−C6 = 1.478(15); dihedral angle C_5,C_6 24.2(6).

imposed by (1), and (3) the EPR features of a biradical, which are governed by the magnitudes of the hyperfine interaction a(^{51}V) and the exchange coupling constant J.

Cyclic voltammetric traces for $\mathbf{5}^{2\bullet}$ are shown in Figure 3; the pertinent data are given in the caption. Relative to the parent complex **1**• the derivative **8**• exhibits an anodic and the derivative $\mathbf{5}^{2\bullet}$ a cathodic shift of the redox potential $E_{1/2}$(+/0). This is in line with the electron-

(13) Negishi, E. I. *Acc. Chem. Res.* **1982**, *15*, 340. Negishi, E. I. In *Organozinc Reagents. A Practical Approach*; Knochel, P., Jones, P.; Eds.; Oxford University Press: Oxford, U.K., 1999; Chapter 11.

(14) Charbonneau, G. P.; Delugeard, Y. *Acta Crystallogr., Sect. B* **1977**, *33*, 1586.

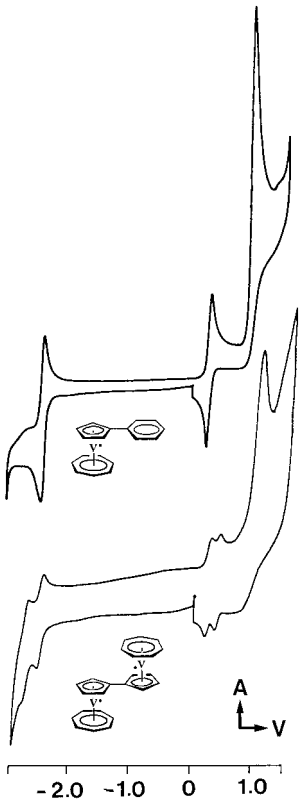

Figure 3. Cyclic voltammograms for [5-5]bitrovacene $\mathbf{5}^{2\bullet}$ and phenyl−[5]trovacene $\mathbf{8}^{\bullet}$ in DME/t-Bu_4NClO_4 at −40 °C and 100 mV/s. Compound $\mathbf{5}^{2\bullet}$: $E_{1/2}(2+/+) = 0.364$ V, $\Delta E_p = 64$ mV, $r = 1$; $E_{1/2}(+/0) = 0.217$ V, $\Delta E_p = 62$ mV, $r = 1$; $E_{1/2}(0/-) = -2.484$ V, $\Delta E_p = 60$ mV, $r = 1$; $E_{1/2}(-/2-) = -2.708$ V, $\Delta E_p = 60$ mV, $r = 1$. Compound $\mathbf{8}^{\bullet}$: $E_{1/2}(+/0) = 0.297$ V, $\Delta E_p = 59$ mV, $r = 1$; $E_{1/2}(0/-) = -2.458$ V, $\Delta E_p = 59$ mV, $r = 1$. Compound $\mathbf{1}^{\bullet}$:[11] $E_{1/2}(+/0) = 0.26$ V, $\Delta E_p = 64$, $r = 0.9$; $E_{1/2}(0/-) = -2.55$ V, $\Delta E_p = 66$ mV, $r = 1$.

accepting properties of the phenyl substituent and the electron-donating nature of the [5]trovacenyl unit. Consequently, reduction of $\mathbf{8}^{\bullet}$ is somewhat easier (anodic shift) than that of the parent $\mathbf{1}^{\bullet}$. As opposed to oxidation, reduction of binuclear $\mathbf{5}^{2\bullet}$ fails to show a significant shift in redox potential relative to $\mathbf{1}^{\bullet}$. The lack in parallelism of the shifts pertaining to oxidation and reduction may be traced to the fact that the cathodic shift expected for substitution of H by an electron-releasing trovacenyl group is balanced by electron delocalization, which stabilizes the mixed-valence binuclear species $\mathbf{5}^{\bullet-}$ (anodic shift). This effect should be more pronounced for the radical anion $\mathbf{5}^{\bullet-}$ compared to the radical cation $\mathbf{5}^{\bullet+}$ in view of the expanded nature of the vanadium orbitals in the former, compared to their contracted nature in the latter. This notion also serves to explain the gradation in redox splittings for $\mathbf{5}^{2\bullet}$, which amount to $\delta E_{1/2}[(2+/+),(+/0)] = 147$ mV and $\delta E_{1/2}\{(0/-),(-/2-)] = 224$ mV, respectively. Since oxidation and reduction of trovacene must be regarded as metal-centered,[11] the extent of intramolecular interaction obviously depends on complex charge, since the latter governs the extension of the V($3d_{z^2}$) orbitals which comprise the HOMOs of the trovacene units.[21b]

Neither redox splitting is sufficiently large, however, to permit the generation of the mixed-valence species $\mathbf{5}^{\bullet+}$ or $\mathbf{5}^{\bullet-}$ for EPR examination in the absence of considerable concentrations of the homovalent entities, $\mathbf{5}^{2+} + \mathbf{5}^{2\bullet}$ and $\mathbf{5}^{2-} + \mathbf{5}^{2\bullet\cdot\cdot}$, respectively. Rather than trying to monitor communication by means of the rate of intramolecular electron transfer in $\mathbf{5}^{\bullet+}$ or $\mathbf{5}^{\bullet-}$, we therefore reverted to exchange coupling J in the neutral biradical $\mathbf{5}^{2\bullet}$ as a gauge to study the intermetallic interaction. This also has the advantage that barriers set up by solvent reorganization and/or counterion movement, accompanying intramolecular ET in $\mathbf{5}^{\bullet+}$ or $\mathbf{5}^{\bullet-}$, are absent in neutral $\mathbf{5}^{2\bullet}$.

The EPR spectra of $\mathbf{5}^{2\bullet}$ in fluid and rigid solution are depicted in Figure 4; the parameters are found in the caption. It is immediately apparent that the spectrum of the biradical $\mathbf{5}^{2\bullet}$ conforms to the "fast exchange limit",[15] since the hyperfine pattern signalizes electron spin coupling to two nuclei ^{51}V ($I = {}^7/_2$), the splitting corresponding to half the value observed for the mononuclear complexes $\mathbf{1}^{\bullet}$ ($a(^{51}V) = 6.98$ mT) and $\mathbf{8}^{\bullet}$ ($a(^{51}V) = 7.18$ mT). The slightly larger value for $\mathbf{8}^{\bullet}$, compared to $\mathbf{1}^{\bullet}$, results from the electron-accepting properties of the phenyl substituent which causes electron withdrawal from the e_2 MO into the periphery, thereby slightly increasing the positive partial charge on the central metal atom with concomitant contraction of the virtually nonbonding SOMO a_1 (>90% V($3d_{z^2}$[21b])). The argument matches that given above to rationalize the anodic shift $E_{1/2}[\mathbf{8}^{\bullet};+/0] - E_{1/2}[\mathbf{1}^{\bullet};+/0]$. As to the value of the exchange coupling constant J, all that can be inferred from the EPR spectrum of $\mathbf{5}^{2\bullet}$ is the relation $J(\mathbf{5}^{2\bullet}) \geq 1.5$ cm^{-1}. This is because the cases "small", "intermediate", and "fast" exchange[15] are tied to the relative magnitudes of J and $a(^{51}V)$,[16] the latter amounting to 65×10^{-4} cm^{-1} (7 mT) for $\mathbf{1}^{\bullet}$. The lower limit $J(\mathbf{5}^{2\bullet}) \geq 1.5$ cm^{-1} represents the ratio $J/a = 230$, i.e., $J \gg a$. This lower limit we have derived from the fact that for $J \geq 1.5$ cm^{-1} the goodness of spectral simulation[17] is invariant to changes of the input parameter J.

The biradical character of $\mathbf{5}^{2\bullet}$ is also illustrated by the detection of a "half-field signal" at $g \approx 4$ in the rigid solution spectrum. Observation of this type of signal for weakly interaction V(d^5) centers is the exception rather than the rule because the inherently low intensity of the spin-forbidden $\Delta M_s = 2$ transition is spread over 15 ^{51}V hyperfine components. In the present case, the

(15) In the context of magnetic exchange, the terms "time scale", "slow", and "fast" are used in a physically descriptive sense.

(16) For a clear exposition of the factors governing the hyperfine pattern in the EPR spectra of biradicals, see: Atherton, N. M. *Principles* of *Electron Spin Resonance*; Ellis Horwood: Chichester, U.K., 1993; Chapter 6.

(17) For details of the simulation see ref 1.

(18) Chasteen, N. D.; Belford, R. L. *Inorg. Chem.* **1970**, *9*, 169.

(19) Adoption of a trans disposition of the trovacene units of $\mathbf{5}^{2\bullet}$ in an isotropic medium is favored by intramolecular dipole forces. Note, however, that the isoelectronic diradical dication {(μ-η^6:η^6-biphenyl)-bis[(η^6-benzene)chromium]}$^{2\bullet 2+}$ ($\mathbf{4}^{2\bullet 2+}$) has a twisted structure which probably arises from ion pairing.[8d]

(20) Kahn, O. *Molecular Magnetism*; VCH: Weinheim, Germany, 1993; Chapter 6.

(21) (a) Rettig, M. F. in *NMR of Paramagnetic Molecules: Principles and Applications*; LaMar, G. N., Horrocks, W. DeW., Jr., Holm, R. H., Eds.; Academic Press: New York, 1973; Chapter 6. (b) Rettig, M. F.; Stout, C. D.; Klug, A.; Farnham, P. *J. Am. Chem. Soc.* **1970**, *92*, 5100. (c) Elschenbroich, C.; Möckel, R.; Zenneck, U.; Clack, D. W. *Ber. Bunsen-Ges. Phys. Chem.* **1979**, *83*, 1008.

(22) (a) McCleverty, J. A.; Ward, M. D. *Acc. Chem. Res.* **1998**, *31*, 842. (b) Ward, M. D. *Chem. Soc. Rev.* **1995**, 121.

(23) Atzkern, H.; Bergerat, P.; Bernda, H.; Fritz, M.; Hiermeier, J.; Hudeczek, P.; Kahn, O.; Köhler, F. H.; Paul, M.; Weber, B. *J. Am. Chem. Soc.* **1995**, *117*, 997.

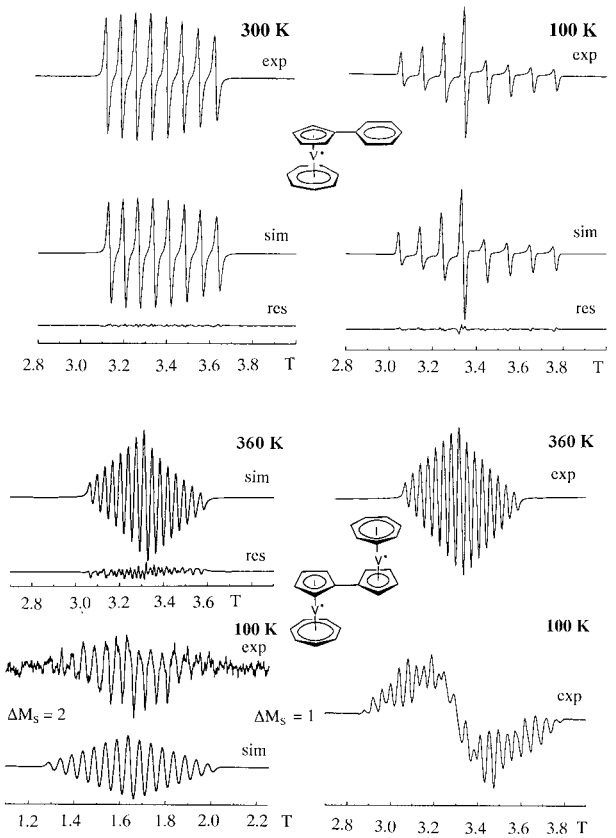

Figure 4. EPR spectra of [5-5]bitrovacene $\mathbf{5}^{2\bullet}$ and phenyl−[5]trovacene $\mathbf{8}^{\bullet}$ in fluid solution (toluene) and in rigid solution (toluene). $\mathbf{8}^{\bullet}$: $\langle g\rangle = 1.9829$, $g_{\|} = 2.0020$, $g_{\perp} = 1.9733$, $a(^{51}\mathrm{V}) = -7.18$ mT, $A_{\|}(^{51}\mathrm{V}) = -1.02$ mT, $A_{\perp} = -10.26$ mT. Line width parameters in the simulation: $b = -0.55$, $c = 1.91$, $d = 0$. $\mathbf{5}^{2\bullet}$: $a(^{51}\mathrm{V}) = -7.18$ mT, $\langle g\rangle = 1.9816$, $J = -1.5$ cm^{-1}, $b = -0.15$, $c = -0.10$, $d = -0.18$. exp = experimental, sim = simulated, res = residual.

splitting in the $\Delta M_s = 2$ multiplet amounts to 4.9 mT, which corresponds to $A_{\perp}(^{51}\mathrm{V})/2$. The $\Delta M_s = 1$ signal at $g \approx 2$ displays a multiline structure which defies spectral simulation. The complication arises from the fact that the anisotropies of the **g**, hyperfine, and zero-field splitting tensors are of similar magnitude. As in the case of the symmetrical isomer $\mathbf{4}^{2\bullet}$,[8d] a value for the ZFS parameter D can be extracted from the rigid solution spectrum, however, assuming that the distance between the two outermost lines (low field, high field, respectively) is equal to $2D + 14[a(^{51}\mathrm{V})]$. The value $D = 150$ G (0.014 cm^{-1}) thus obtained for $\mathbf{5}^{2\bullet}$ is slightly smaller than the respective parameter for $\mathbf{4}^{2\bullet}$, $D = 0.0154$ cm^{-1}; when the point-dipole approximation is employed,[18] the D value translates into an inter-vanadium distance R(V···V) of 5.70 Å for $\mathbf{5}^{2\bullet}$, compared to 5.40 Å for $\mathbf{4}^{2\bullet}$. R(V···V) for $\mathbf{5}^{2\bullet}$ in rigid solution, calculated in this fashion, closely matches the value of 5.50 Å pertaining to the single crystal. Therefore, $\mathbf{5}^{2\bullet}$, like $\mathbf{4}^{2\bullet}$, in rigid solution adopts the trans conformation.[19] The gradation R(V···V,$\mathbf{5}^{2\bullet}$) > R(V···V,$\mathbf{4}^{2\bullet}$), inferred from the EPR spectra, conforms with the fact that the metal−ring-centroid distances in π-perimeter complexes increase with decreasing ring size.

Since the EPR spectrum of $\mathbf{5}^{2\bullet}$ only yielded a lower limit for the exchange coupling constant J, $\mathbf{5}^{2\bullet}$ was subjected to a determination of its bulk magnetic susceptibility χ. A plot of χ^{-1} versus T is shown in Figure

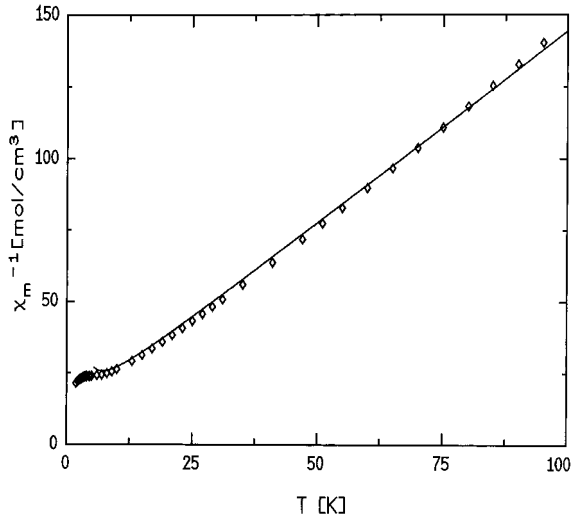

Figure 5. Temperature dependence of the inverse magnetic susceptibility χ^{-1} for [5-5]bitrovacene ($\mathbf{5}^{2\bullet}$). For parameters and fitting procedure, see text.

5. The data of the magnetic susceptibility have been fitted according to the isotropic Heisenberg model for a dimer antiferromagnetic $S = {}^1/_2$ spin system[20] with $\chi_m = 2Ng^2\mu_B{}^2\{k\mathrm{T}[3 + \exp(-J/kT)]\}^{-1}$. This led to a value for the exchange parameter of $J/k = -4.0(1)$ K corresponding to $J = -2.8$ cm^{-1}. The significant deviations from the classical Heisenberg model observed at low temperatures ($T < 6$ K) may be caused by small but finite interdimer exchange interaction. Besides, at higher temperatures ($T > 50$ K) the data could be fitted applying the Curie−Weiss law with the parameters for the Curie−Weiss temperature and the Curie−Weiss constant $\Theta_p = -5.5(5)$ K and $C = 0.72(5)$ cm^3 K/mol, respectively. The derived value of the magnetic moment $\mu_c = 2.40(5)$ μ_B corresponds to $\mu_V = 1.70(3)$ μ_B per vanadium atom. The value of the exchange interaction J, obtained for the biradical $\mathbf{5}^{2\bullet}$, at first sight appears surprisingly small considering the fact that two V(d^5) atoms are connected by a conjugated π-system, the μ-η^5:η^5-fulvalenediyl bridge, which is devoid of spacer atoms between the constituting cyclopentadienyl units. A closer look at the mechanisms of metal−ligand spin transfer in this class of complexes is called for, however. As has been discussed previously, spin density at α-positions in the periphery of an M(d^5)-coordinated π-perimeter probably arises from the aggregate action of at least two mechanisms,[21] each of which lacks high efficiency. Typically, the spin population $\rho_{1s}(^1\mathrm{H})$ at the hydrogen atom of the η^5-C_5H_5 ligand in trovacene amounts to only 0.0035, as inferred from the isotropic hyperfine coupling constant $a(^1\mathrm{H_{Cp}}, \mathbf{1}^{\bullet}) = 0.18$ mT;[21b] the small value of $J = -2.78$ cm^{-1} for [5-5]bitrovacene is therefore plausible. Much larger exchange interactions are observed when the magnetic metal orbitals are of correct symmetry to engage in d(π)−p(π) overlap with the bridging ligand[22] rather than being orthogonal as in the present case of M(d^5) sandwich complexes. This also applies to exchange interactions between metallocenes of the configuration $e_{2g}{}^2a_{1g}{}^1$ (vanadocene), $e_{2g}{}^3a_{1g}{}^1$ (chromocene), $e_{2g}{}^4a_{1g}{}^2e_{1g}{}^1$ (cobaltocene), and $e_{2g}{}^4a_{1g}{}^2e_{2g}{}^2$ (nickelocene), which place spin density in molecular orbitals with sizable π-ligand contribution.[23] The small magnitude of J for trovacene-based oligoradicals is,

however, instrumental in the application of fluid solution EPR to study intermetallic communication because it is only if the relation $J \lesssim 100$ ($a(^{51}V) = 65 \times 10^{-4}$ cm^{-1}) holds that valuable information can be derived from the hyperfine pattern. Fluid solution EPR of trovacene oligoradicals therefore complements bulk susceptibility studies in that by the former very weak intermetallic interactions can be monitored.[1] In this pursuit, the value for J determined here for $\mathbf{5}^{2\bullet}$ constitutes the standard against which bitrovacenes, containing spacers between the sandwich units, must be measured. Work along these lines to be reported shortly includes the use of sp^2-hybridized boron[10a] and of ethane- and ethylene-based bridges,[10b] as well as the study of bis-, tris-, and tetrakis(trovacenyl) derivatives of benzene[10c] and naphthalene.[10a]

Experimental Section

Chemical manipulations and physical measurements were carried out using techniques and instrumentes specified previously.[24] Magnetic susceptibility was studied with a SQUID susceptometer (Quantum Design) in the temperature range 1.4−300 K. Trovacene **1**[25] and Pd(dppf)Cl_2[26] were prepared as described in the literature. Anhydrous zinc chloride was obtained by melting $ZnCl_2 \cdot 4H_2O$ in vacuo.

[5-5]Bitrovacene ($\mathbf{5}^{2\bullet}$). Trovacene (**1**; 281 mg, 1.36 mmol), dissolved in 50 mL of diethyl ether, is metalated by 0.85 mL of a solution (1.6 M) of n-BuLi in hexane during 10 h at room temperature. The diethyl ether is removed in vacuo and replaced by 50 mL of tetrahydrofuran. Pd(dppf)Cl_2 (25 mg, 0.034 mmol) and iodocyclohexane (0.086 mL, 0.66 mmol) are dissolved in 20 mL of tetrahydrofuran and stirred for 5 min. This solution is added slowly at −50 °C to a solution of ([5]-trovacenyl)lithium followed by 1 h at room temperature and refluxing for 12 h. The solvents are evaporated in vacuo; the residue is dissolved in benzene and subjected to column chromatography (Al_2O_3, 0% H_2O, benzene). The first band contains trovacene and traces of cyclohexyltrovacene; the second band consists of [5-5]bitrovacene (**5**), which is recrystallized from toluene (10 mL). Yield: 140 mg (25%) of violet crystals. MS (EI, 70 eV): *m*/*z* (relative intensity) 412 (M^+, 100), 319 ($M^+ - C_7H_9$, 46), 292 (μ, 11), 267 (μ, 10), 206 (M^{2+}, 13). IR (KBr): 3044 w, **1828**, *1756*, 1634, 1576, m, br, 1500−1388 m, 777 sst, br, 450 w, 430 sst. Anal. Calcd. for $C_{24}H_{22}V_2$ (412.32): C, 69.91; H, 5.38. Found: C, 69.79; H, 5.80. For EPR and CV see text.

Phenyl−[5]trovacenyl ($\mathbf{8}^{\bullet}$). Trovacene (**1**; 300 mg, 1.4 mmol) in 50 mL of diethyl ether is metalated by 0.9 mL of a solution (1.6 M) of n-BuLi in hexane during 10 h at room temperature. To this are added at room temperature 1.6 mL of a solution (0.9 M) of anhydrous $ZnCl_2$ in tetrahydrofuran. Iodobenzene (142 mg, 0.7 mmol) and Pd(dppf)Cl_2 (5 mg, 1 mol %) are dissolved in 20 mL of tetrahydrofuran and stirred for 30 min at room temperature. This solution is added to the solution of [5]trovacenyl−ZnCl, and the mixture is refluxed for 20 min. After the solvents are removed in vacuo and the residue is taken up in 5 mL of benzene, separation is effected by column chromatography (Al_2O_3, 0% H_2O, benzene/petroleum ether 1:20). Trovacene is followed by phenyl−[5]trovacene which can be recrystallized from 3 mL of toluene. Yield: 176 mg (45%) of violet platelets. MS (ET, 70 eV): *m*/*z* (relative intensity) 283 (M^+, 100), 205 ($M^+ - C_6H_6$, 10), 192 ($M^+ - C_7H_7$, 12), 116 ($C_5H_5V^+$, 11), 51 (V^+, 33). IR (KBr): 3058 w, 1800−1600 w, 1600−1450 m, 779 sst, 698 sst, 462 w, 450 m, 435 m, 409 w. Anal. Calcd for $C_{18}H_{16}V$ (283.27): C, 76.32; H, 5.69. Found: C, 75.91; H, 5.75. For EPR and CV see text.

X-ray Crystallographic Study of $\mathbf{5}^{2\bullet}$ and $\mathbf{8}^{\bullet}$. Data were collected by means of a STOE IPDS system employing Mo Kα radiation (λ = 0.710 73 Å). The structures have been solved by direct methods[27a] and refined[27b] on F^2 values using a full-matrix least-squares procedure; all non-hydrogen atoms were refined anisotropically. Hydrogen atoms were included at calculated positions and refined on the basis of a riding model. $\mathbf{5}^{2\bullet}$ possesses a crystallographic center of inversion. $\mathbf{8}^{\bullet}$ features two independent molecules in the asymmetric unit. Crystal data for $\mathbf{5}^{2\bullet}$: $C_{24}H_{22}V_2$, M_r = 412.3, crystal size 0.30 × 0.20 × 0.10 mm^3; monoclinic, space group $P2_1/n$, Z = 2; a = 10.447(2) Å, b = 8.089(1) Å, c = 10.911(2) Å, β = 102.25(3)°, V = 901.0(3) $Å^3$, d_{calcd} = 1.520 Mg/m^3, $F(000)$ = 424; T = 243(2) K; θ range 2.45−25.91°, index ranges $-12 \le h \le 12$, $-9 \le k \le 9$, $-13 \le l \le 13$, 6791 reflections collected, 1741 independent reflections (R_{int} = 0.0613), 1171 observed reflections ($I > 2\sigma(I)$); R1 = 0.0321, wR2 = 0.0673; largest difference peak/hole +0.0336/−0.227 e $Å^{-3}$. Crystal data for $\mathbf{8}^{\bullet}$: $C_{18}H_{16}V$, M_r = 283.25, crystal size 0.30 × 0.20 × 0.05 mm^3; monoclinic, space group $P2_1$, Z = 4; a = 10.768(3) Å, b = 7.851(2) Å, c = 16.189(6) Å, β = 97.53(3)°, V = 1356.7(7) $Å^3$, d_{calcd} = 1.387 Mg/m^3, $F(000)$ = 588; T = 190(2) K; θ range 2.15−22.00°, index ranges $-11 \le h \le 11$, $-8 \le k \le 8$, $-17 \le l \le 17$; 5929 reflections collected, 3298 independent reflections (R_{int} = 0.1250), 2233 observed reflections ($I > 2\sigma(I)$); R1 = 0.0736, wR2 = 0.1930; largest difference peak/hole +0.927/−0.552 e $Å^{-3}$.

Acknowledgment. This work has been supported by the Volkswagen Foundation and the Fonds der Chemischen Industrie.

Supporting Information Available: Tables giving crystal data and details of the structure determination, positional and thermal parameters, and all bond distances and angles for **5** and **8**. This material is available free of charge via the Internet at http://pubs.acs.org.

OM9902232

(24) Elschenbroich, C.; Voss, S.; Schiemann, O.; Lippek, A.; Harms, K. *Organometallics* **1998**, *17*, 4417.
(25) King, R. B. *J. Am. Chem. Soc.* **1959**, *81*, 5263.
(26) Hayashi, T.; Konishi, M.; Kumada, M. *Tetrahedron Lett.* **1979**, *21*, 1871.
(27) (a) Sheldrick, G. M. SHELXS-97-2, Program for the Solution of Crystal Structures; Göttingen, Germany, 1998. (b) Sheldrick, G. M. SHELXL-97-2, Program for the Refinement of Crystal Structures; Göttingen, Germany, 1998.